Role of Gradation Curve in Description of Mechanical Behavior of Unsaturated Soils

G. N. Pande[1]; S. Pietruszczak[2]; and Min Wang, Ph.D.[3]

Abstract: This paper presents a framework for the incorporation of the gradation curve in the description of mechanical behavior of unsaturated soils at low to medium degrees of saturation. Unsaturated soils have self-equilibrating initial stresses arising from surface tension forces acting on water menisci, which depend on the microstructure of saturation, particle surface contact characteristics, and pore size distribution (POSD). The latter, in turn, can be related to gradation curve. Unsaturated soil is treated here as a three-phase composite material, and its mechanical response is derived from that of its constituents: soil skeleton, water, and air. This approach leads to an analytical expression for the soil water retention curve (SWRC) in which the critical parameter to be determined is the water menisci area per unit volume (S_{wma}) of the soil. This parameter can be identified from the gradation curve using well-established methodologies in soil science and agricultural engineering. Numerical simulations of triaxial tests show that deformation and strength of unsaturated soils, at a given degree of saturation and confinement, are influenced by the gradation curve, and its incorporation in the description of mechanical behavior of unsaturated soils is rational. **DOI: 10.1061/(ASCE)GM.1943-5622.0001551.** *© 2019 American Society of Civil Engineers.*

Author keywords: Unsaturated soils; Gradation curve; Pore-size distribution; Soil water retention characteristics.

Introduction

There has been enormous interest among researchers and engineers in the last two decades in developing constitutive models for unsaturated geomaterials. This seems to have been prompted by plans in many countries for development of infrastructure, generation of renewable and nonrenewable energy, geological disposal of nuclear waste, and so on. Many theories to characterize the mechanical response, methodologies for laboratory testing, and new equipment to measure suction pressures have been developed. Instruments to monitor in-situ behavior of unsaturated soils have also been developed and used in a few cases. Most publications attempt to extend standard soil mechanics and its long-established fundamental principle of effective stress for saturated soils to unsaturated soils. A number of textbooks dedicated to the mechanics of unsaturated soils have been published (Fredlund and Rahardjo 1993; Ning and Likos 2004; Ng and Menzies 2007). Until recently, most books (e.g., Barnes 2010; Craig 2013) had very limited information on unsaturated soils, usually contained in the chapter related to compaction or highway engineering.

It is admitted that the mechanical response of unsaturated soils is more complicated than that of fully saturated or dry soils. This is mainly due to the complexity of the microstructure of saturation. However, unsaturated soil is not a new material but a state of soil influenced by variation in the degree of saturation. For solving practical engineering problems and in a bid to match experimentally observed response, an additional parameter, that is, matric suction, considered as an independent state variable, was proposed in the so-called basic Barcelona model (BBM) (Alonso et al. 1990). This model has been subsequently extended and modified by many researchers (Khalili and Khabbaz 1998; Wheeler et al. 2002; Pedroso and Farias 2011), though questions relating to its validity have also been raised (Baker and Frydman 2009; Zhang 2016; Pande and Pietruszczak 2015). A significant experimental effort has been devoted to validation of this approach that has included testing various types of soils under constant suction (Chen et al. 1999; Pereira and Fredlund 2000; Lim and Miller 2004; Schanz 2007). In order to achieve better correlation with experiments, it was proposed to incorporate the soil water retention curve (SWRC) (Gallipoli et al. 2003a; Wheeler et al. 2003; Khalili et al. 2008) in addition to suction. However, it was then realized that the SWRC also depends on changes in void ratio or strain. This has led many researchers to develop semiempirical expressions of strain-dependent SWRCs involving the introduction of additional parameters describing its evolution (Gallipoli et al. 2003b; Tarantino 2009; Dieudonné et al. 2013; Khoshghalb et al. 2015; Pasha et al. 2017).

In this paper, gradation curve or particle size distribution (PSD) is proposed as an alternative input to describe the mechanical response of unsaturated soils. From PSD, a pore size distribution (POSD) as well as SWRC can be obtained (Gupta and Larson 1979; Arya and Paris 1981; Haverkamp and Parlange 1986; Frydman and Baker 2009; Imre et al. 2012; Beckett and Augarde 2013; Hu et al. 2013). Moreover, from POSD, it is also possible to compute strain-dependent SWRC based on certain assumptions relating to changes in POSD due to volumetric strains. Tests to obtain SWRC in the laboratory or in field are time consuming and expensive. Thus, the methodology presented here may be considered a pragmatic approach for the analysis of real engineering structures.

The scope of this paper is restricted to soils that are inert to chemical interaction and are at a low to medium degree of saturation. The section "Microstructure of Saturation in Soils" briefly discusses various types of microstructure that may arise at different

[1]Professor Emeritus, Zienkiewicz Centre for Computational Engineering, Swansea Univ., Swansea SA1 8EN, UK (corresponding author). Email: g.n.pande@swansea.ac.uk

[2]Professor, Dept. of Civil Engineering, McMaster Univ., Hamilton, ON, Canada L8S 4L7. Email: pietrusz@mcmaster.ca

[3]Project Engineer, Rockfield Software Ltd., Kings Rd., Swansea SA1 8AS, UK. Email: sacewangmin@gmail.com

Note. This manuscript was submitted on February 3, 2018; approved on June 11, 2019; published online on December 3, 2019. Discussion period open until May 3, 2020; separate discussions must be submitted for individual papers. This paper is part of the ***International Journal of Geomechanics***, © ASCE, ISSN 1532-3641.

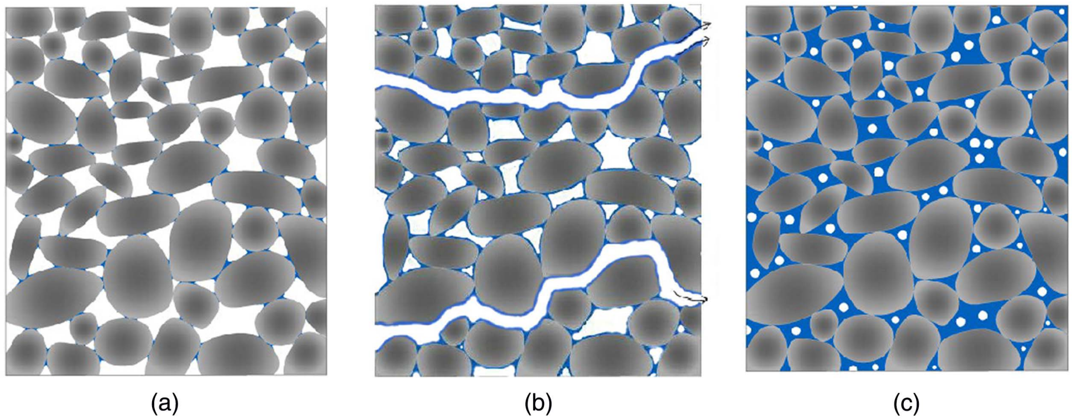

Fig. 1. Schematic representation of microstructure of saturation: (a) Type A: air phase continuous but water phase discontinuous ($S_r < 0.25$, approximately); (b) Type B: water and air phases both continuous ($0.25 < S_r < 0.75$, approximately); and (c) Type C: high degree of saturation-water phase continuous but air phase discontinuous ($S_r > 0.75$, approximately).

degrees of saturation. This is important because the response of unsaturated soils changes depending not only on degree of saturation but also the microstructure of saturation. The section "Stress–Strain Behavior of Unsaturated Soil Treated as a Composite Material" deals with the development of the stress–strain relation. The response is defined in terms of properties of constituents, that is, soil skeleton, water, and air, and their microstructural arrangement. A notion of specific water menisci area per unit volume (S_{wma}) is introduced and, an analytical expression relating it to suction is obtained. The section "Assessment of SWRC for Assemblages of Monospheres" presents an assessment of SWRC for monospheres with four different packings. (This assumption is not new, given that it is embedded in geotechnical engineering practice in the interpretation of gradation curve and the evaluation of POSD.) This is done for two cases of microstructure of saturation, that is, discontinuous menisci formed at the interparticle contacts (pendular menisci) and a continuous film of water adhering to grain boundaries. The section "Computation of SWRC from PSD or POSD" gives a brief review of research linking PSD and POSD to SWRC in the fields of agricultural engineering, soil science and agronomy, and so on, to obtain SWRC from PSD and POSD. The procedure is then extended to obtain strain-dependent POSD as well as SWRC. The last section gives results of simulations of triaxial tests on two hypothetical soils that have the same porosity and initial degree of saturation but different gradation curves. Significantly different response is observed depending on gradation curves. Conclusions and recommendations for future experimental research are given in "Conclusions."

Microstructure of Saturation in Soils

From the experimental evidence based on X-ray computerized tomography (CT) studies (Romero and Simms 2008; Lourenço et al. 2012; Shin et al. 2013), it seems that a sample of unsaturated soil is unlikely to be homogenous with reference to its microstructure of saturation. Concave as well as convex water menisci, discontinuities, and dry and wet patches are observed in the same sample (Lourenço et al. 2012). At the same time, the degree of saturation evolves during the test and thus the microstructure of saturation changes broadly depending on the type of soil that is, clay, silt, or sand. Thus, a sample of unsaturated soil can be treated as macroscopically homogenous only in an average sense.

From the point of view of numerical simulations, three different types of microstructures of saturation can be visualized in unsaturated soils (Pietruszczak and Pande 1991, 1995, 1996). These are shown in Fig. 1, where approximate range of degree of saturation (S_r) is also indicated. In Type A, water adheres to contacts between the grains and is discontinuous, whereas the air phase is continuous. In Type B, the water phase and air phase are both continuous, whereas in Type C, only the water phase is continuous. This paper is restricted to microstructures of saturation of Types A and B. These types of saturation are likely to be applicable to a majority of cases.

Stress–Strain Behavior of Unsaturated Soil Treated as a Composite Material

For soils with a microstructure of saturation of either Type A or B, soil behavior can be described by the constitutive relation of the soil skeleton subjected to additional confining pressure due to suction. The assessment of suction for these types of microstructure is addressed in the section "Assessment of SWRC for Assemblages of Monospheres."

The mathematical formulation for the microstructure of saturation of Type B was discussed by the first two authors in a conference paper (Pietruszczak and Pande 1995). However, it is briefly described here, albeit in a slightly different form, for the sake of completeness and continuity.

Unsaturated soil samples are three-phase composites comprising skeleton, water, and air as constituents. The average macroscopic stress σ_{ij} within a representative volume V may be defined as

$$\sigma_{ij} = \frac{1}{V}\left(\int_{V_S} \bar{\sigma}^s_{ij} dV_S + \int_{V_V} \bar{p}\delta_{ij} dV_V\right) \tag{1}$$

where $\bar{\sigma}^s_{ij}$ = stress field in the skeleton; $\bar{p}$ = pressure field in the voids measured above a threshold value (atmospheric pressure); V_S = volume of solid; and V_V = volume of voids. The integrals appearing in Eq. (1) are proportional to the respective volume averages of both fields, that is

$$\sigma_{ij}^{s} = \frac{1}{V_S}\int_{V_S} \bar{\sigma}_{ij}^{s} dV_S; \qquad p = \frac{1}{V_V}\int_{V_V} \bar{p} dV_V \tag{2}$$

where σ_{ij}^{s} = *average* stress in the skeleton; and p = average excess pressure in the voids. Substitution of Eq. (2) in Eq. (1) leads to

$$\sigma_{ij} = (1-n)\sigma_{ij}^{s} + np\delta_{ij} \tag{3}$$

where $n = V_V/V$ is the porosity of the sample.

Consider now the interconnected voids as a free body. The average pressure p may be defined as

$$p = \frac{1}{V_V}\left(\int_{V_W} \bar{p}_w dV_w + \int_{V_a} \bar{p}_a dV_a - \int_{S_m} T dS_m\right) \tag{4}$$

where $\bar{p}_w$ and $\bar{p}_a$ = excess pressure in the water (occupying volume V_w) and air (of volume V_a), respectively; T = surface tension force (per unit length of the air-water meniscus); and S_m = surface area of air-water menisci. Denoting by p_w and p_a the volume averages of $\bar{p}_w$ and $\bar{p}_a$, Eq. (4) may be expressed as

$$p = S_r p_w + (1-S_r)p_a - \frac{TS_m}{V_V} \tag{5}$$

In the microstructure of Type B being discussed here, the grains are considered to be in a direct contact with water; therefore, $p = p_w$ so that Eq. (5) reduces to

$$p_a - p_w = \frac{TS_m}{V_V(1-S_r)} \tag{6}$$

Dividing both terms of the fraction on the right-hand-side by V, Eq. (6) can be expressed as

$$p_S = p_a - p_w = \frac{S_{\mathrm{wma}}T}{n(1-S_r)} \tag{7}$$

where $S_{\mathrm{wma}} = S_m/V$ is the specific water menisci area. The previous equation is an analytical expression of SWRC, and the parameter S_{wma} can be determined either from the gradation curve of the soil or from standard physical experiments.

Consider now the constitutive relation governing the behavior of the soil skeleton. Assume that the response of a dry material can be described by an incremental relation

$$\dot{\sigma}_{ij} = \{(1-n)\sigma_{ij}^{S}\}^{\cdot} = D_{ijkl}\dot{\varepsilon}_{kl} \tag{8}$$

For the Type B microstructure, the grains are considered to be surrounded by water at an excess pressure of p_w. In this case, the response of the skeleton alone must be consistent with that given by Eq. (8) and that is

$$\{(1-n)(\sigma_{ij}^{S} - p_w\delta_{ij})\}^{\cdot} = \dot{\sigma}'_{ij} = D_{ijkl}\dot{\varepsilon}_{kl} \tag{9}$$

where σ'_{ij} = effective stress. According to Eq. (9)

$$\sigma'_{ij} = (1-n)\sigma_{ij}^{s} - (1-n)p_w\delta_{ij} \tag{10}$$

The previous definition, combined with Eq. (3), leads to the classical Terzaghi's decomposition (Terzaghi 1936)

$$\sigma_{ij} = \sigma'_{ij} + p_w\delta_{ij} \tag{11}$$

It is important, at this point, to comment on the initial conditions within the specimen. Neglecting the stress due to self-weight and assuming that the air pressure is initially at the atmospheric level, that is, $\sigma_{ij} = 0$ and $p_a = 0$, leads to

$$\sigma'_{ij} = -p_w\delta_{ij} = \beta\delta_{ij}; \quad \beta = \frac{S_{\mathrm{wma}}T}{n(1-S_r)} \tag{12}$$

Thus, initial effective stress in soil samples at zero total stress is given by Eq. (12) above.

Consider now the response of unsaturated soils under undrained conditions. By "undrained conditions," we mean that neither water nor air is allowed to escape from the soil sample under loading or unloading. It is important to point out that the flow of fluids that is, air or water corresponding to any microstructure of saturation, can take place when the gradient of excess pore water or air pressure is generated to establish the flow. In a constant suction test at low to medium degrees of saturation, a continuous flow out of the sample is not possible. Therefore, the response observed is essentially that of the soil skeleton.

In order to define the constitutive relation, express first the volumetric strain rate $\dot{\varepsilon}_{ii} = -\dot{V}_V/V$ (where $\dot{V}_V = \dot{V}_a + \dot{V}_w$) in terms of respective averages $\dot{\varepsilon}_{ii}^{a} = -\dot{V}_a/V_a$ and $\dot{\varepsilon}_{ii}^{w} = -\dot{V}_w/V_w$ as

$$\dot{\varepsilon}_{ii} = n\{(1-S_r)\dot{\varepsilon}_{ii}^{a} + S_r\dot{\varepsilon}_{ii}^{w}\} \tag{13}$$

The stress–strain relations for the constituent materials take the form

$$\dot{\sigma}'_{ij} = D_{ijkl}\dot{\varepsilon}_{kl}; \qquad \dot{p}_w = K_f\dot{\varepsilon}_{ii}^{w}; \qquad \dot{p}_a = K_a\dot{\varepsilon}_{ii}^{a} \tag{14}$$

where K_f = bulk modulus of water and $K_a = p_a + p_0$, with p_o representing the atmospheric pressure. Writing Eq. (7) in incremental form yields

$$\dot{p}_a - \dot{p}_w = \left(\frac{TS_{ws}}{V_V}\frac{V_V}{V_a}\right)^{\cdot} = TS_{\mathrm{wma}}\left(\frac{1}{V_a}\right) = \beta\dot{\varepsilon}_{ii}^{a} \tag{15}$$

At this point, it is convenient to assume that the volumetric strain rates in both constituents can be uniquely derived from $\dot{\varepsilon}_{ii}$, that is

$$\dot{\varepsilon}_{ii}^{a} = B_a\dot{\varepsilon}_{ii}; \qquad \dot{\varepsilon}_{ii}^{w} = B_w\dot{\varepsilon}_{ii} \tag{16}$$

Substituting these relations in Eqs. (14) and (15) yields

$$\dot{p}_a - \dot{p}_w = (K_aB_a - K_fB_w)\dot{\varepsilon}_{ii} = \beta B_a\dot{\varepsilon}_{ii} \tag{17}$$

At the same time, Eqs. (13) and (16) result in

$$\frac{1}{n} = (1-S_r)B_a + S_rB_w \tag{18}$$

Solving now the set of simultaneous Eqs. (17) and (18) yields

$$B_w = \frac{1}{n\{S_r + (1-S_r)\frac{K_f}{K_a-\beta}\}}; \qquad B_a = \frac{K_f}{K_a-\beta}B_w \tag{19}$$

Finally, differentiating Eq. (11) and using Eqs. (17) and (18), the following constitutive relation is obtained:

$$\dot{\sigma}_{ij} = (D_{ijkl} + K_fB_w\delta_{ij}\delta_{kl})\dot{\varepsilon}_{kl} \tag{20}$$

The above relation governs the undrained response of partially saturated soils at medium degrees of saturation. The drained response of unsaturated soil is the same as that of dry soil if the microstructure of Type B is maintained. The framework presented above can be incorporated in any constitutive model for the soil skeleton, and boundary value problems can be solved rationally. The formulation simply extends the applicability of a constitutive model for the soil skeleton to the unsaturated state(s) of the same

Int. J. Geomech., 2020, 20(2): 04019159

soil provided the microstructure of saturation is such that the water as well as air phases are continuous.

Assessment of SWRC for Assemblages of Monospheres

In the previous section, the behavior of unsaturated soil was discussed for the case when both the water and air phases are continuous throughout the soil sample. The formulation incorporates the parameter S_{wma}, which should conceptually be a fraction of the specific surface area (S_s). In this section, some analytical expressions based on Eq. (7) are developed for assemblages of monospheres.

The concept of S_s of a particulate material has been invoked in many branches of engineering and industries such as chemical, pharmaceutical, ceramic, manufacturing, and cement. The main objective there is to define the fineness of materials. A number of methodologies and a wide selection of equipment in the form of particle size and surface area analyzers are readily available for characterization of particle sizes in the range of 10 nm–5 mm.

The general aim of this section is to estimate SWRC for equal-sized particles for two microstructures of saturation:

- Low degree of saturation—pendular water clinging to particles (Type A); that is, air phase continuous and water phase discontinuous
- A layer of water of finite thickness surrounding all particles (Type B)

Low Degree of Saturation—Pendular Water Clinging to Particles (Type A)

Fig. 2(a) shows the water meniscus holding two spherical particles together. This is a classical problem that has a wide range of engineering applications. Particles of different sizes, smooth as well as rough, in contact with each other or having a separation distance, have been considered (Lian et al. 1993; Molenkamp and Nazemi 2003; Mehrotra and Sastry 1980). Many studies deal with computation of the shape and volume of water in the menisci, whereas some recent research (Lian et al. 1993; Molenkamp and Nazemi 2003) deals with suction that can be sustained.

Determination of volume of water requires, in general, a numerical integration. However, if a circular shape of menisci is assumed, an exact analytical expression can be derived (Mehrotra and Sastry 1980). Because our aim here is to obtain an estimate of SWRC, the latter approach is employed, which leads to the following expression for the volume of water in a single contact:

$$V_w = \pi\left[(2R_1^2 + 2R_1 y_0 + y_0^2)x_c - \frac{x_c^3}{3} - (R_1 + y_0)\left(x_c\sqrt{R_1^2 - x_c^2}\right) - R_1^2 \arcsin\left(\frac{x_c}{R_1}\right) - \frac{1}{3}x_c^2(3R - x_c)\right] \tag{21}$$

Suction pressure (p_S) can be computed using equilibrium of forces [Fig. 2(b)] acting on the particles as

$$p_S = \frac{2T(y_0 - y_c \mathrm{Sin}(\beta + \theta))}{y_c^2 - y_0^2} \tag{22}$$

where $x_c = R(1 - \cos\beta)$, $y_c = R\sin\beta$, $y_0 = y_c + R_1(1 - \sin(\beta+\theta))$, $R_1 = R(1 - \cos\beta)/\cos(\beta+\theta)$, with θ being the contact angle and β being the filling angle (see Fig. 2).

From the previous equations, one can compute degree of saturation (S_r) and suction (p_S) for different types of packing, that is, (1) cubic, (2) orthorhombic, (3) tetragonal-sphenoidal, and (4) rhombohedral. These are shown in Fig. 3 and the corresponding number of contacts, volume of unit cell, and porosity are given in Table 1. The variation of S_r with p_s (i.e., SWRC) depends on factors such as diameter of particles (d), contact angle of water (θ), and filling angle (β). Fig. 4 shows the influence of different packing configurations on SWRC with contact angle $\theta = 50°$. Fig. 5 shows SWRCs for different sizes of smooth monospherical grains (tetragonal-spheroidal packing). Here, typical values of mean diameters for sand, silt, and clay have been chosen for illustration. The characteristics correspond to an assemblage with diameters of 0.002–0.02 mm, whereas the contact angles are 0° and 50°. For $\beta = \pi/2 - \theta$, there is $R_1 \to \infty$ so that Eq. (22) becomes singular.

The validity of the pendular microstructure of saturation seems to be within a small range of S_r depending on the type of packing

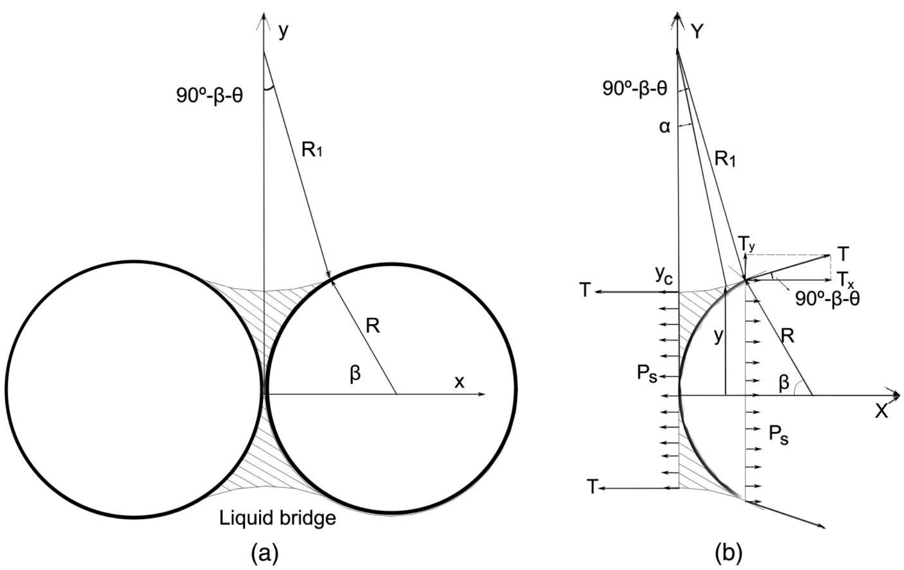

Fig. 2. Interaction between two soil grains, water meniscus, and air: (a) geometry, meniscus assumed circular in shape; and (b) equilibrium of forces along x-axis.

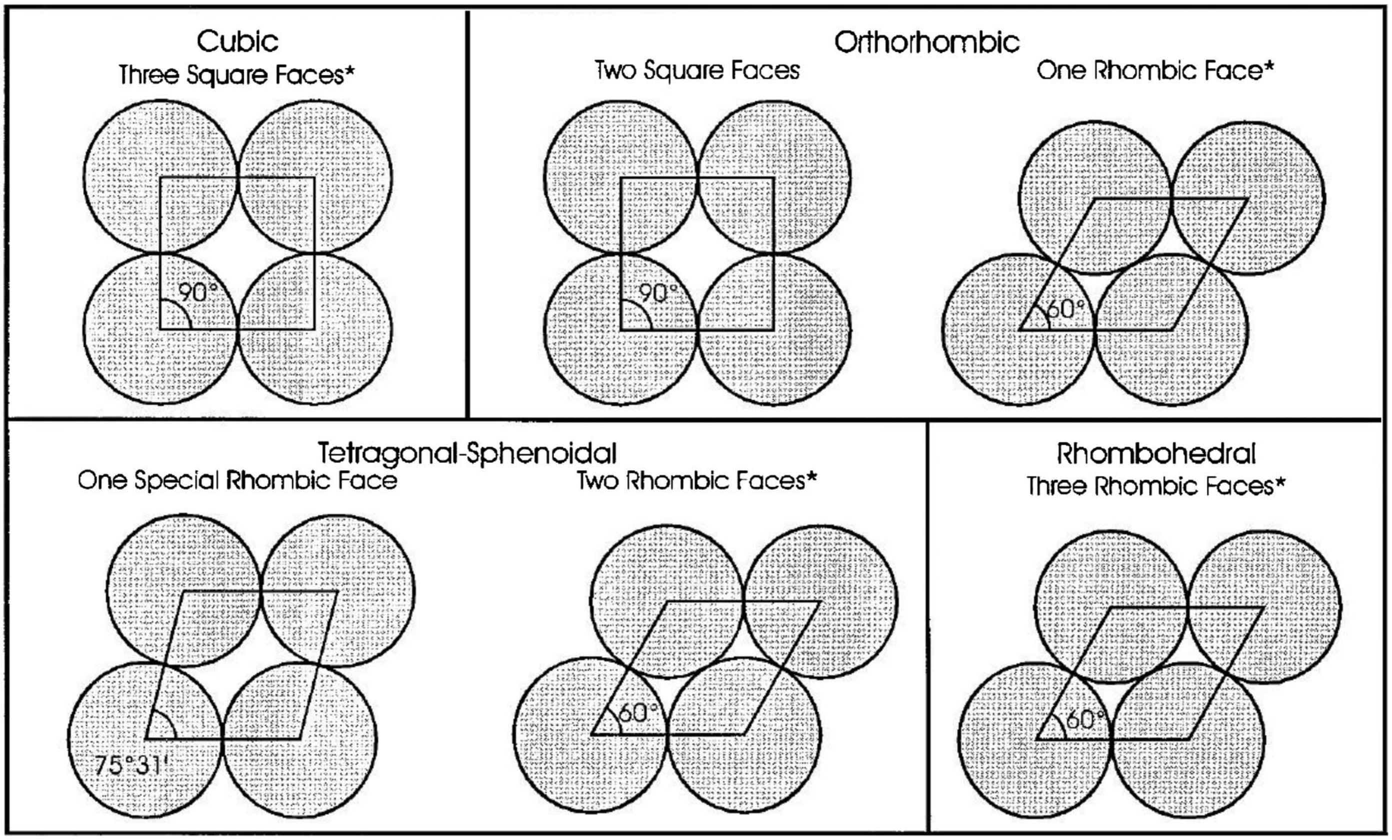

Fig. 3. Four stable, regular packing arrangements illustrated as faces of unit cell (*Indicates critical force). (Reprinted from Cooke and Rowe 1999, © ASCE.)

Table 1. Characteristics of packing of uniform spheres

Packing	Number of contact points (m)	Volume of unit cell	Packing factor	Porosity (%)
Cubic	6	d^3	1	0.4764
Orthorhombic	8	$\sqrt{3}/2d^3$	$\sqrt{3}/2$	0.3954
Tetragonal	10	$0.75d^3$	0.75	0.3019
Rhombohedral	12	$1/\sqrt{2}d^3$	$1/\sqrt{2}$	0.2595

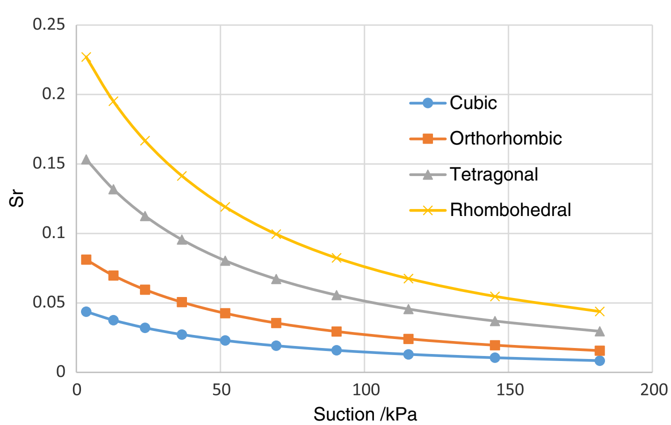

Fig. 4. Computed SWRC for pendular microstructure (Type A) of saturation for different packing of monospheres of diameter 0.002 mm at contact angle 50°.

and contact angle. Further explanation of the range of validity is given toward the end of this section.

Layer of Water of Finite Thickness Surrounding All Particles (Type B)

In this part, we consider a microstructure of saturation of type B, in which a layer of water of finite thickness adheres to the surface of particles. It is obvious that this type of saturation occurs at degrees of saturation higher than those for pendular microstructure discussed previously. A number of analytical studies involving idealized assemblages of particles have been carried out (Taylor 1990; Taylor and Jaffé 1990) in relation to clogging of granular filters by a film of leachate. In these studies, analytical expressions for the porosity and S_s have been derived. Taylor's equations have been modified by other investigators (Cooke and Rowe 1999; Yu and Kerry Rowe 2012) to account for overlaps of fluid or solid caps, initially ignored by Taylor. Here, we employ the original Taylor expressions, in view of their simplicity, with the aim of getting

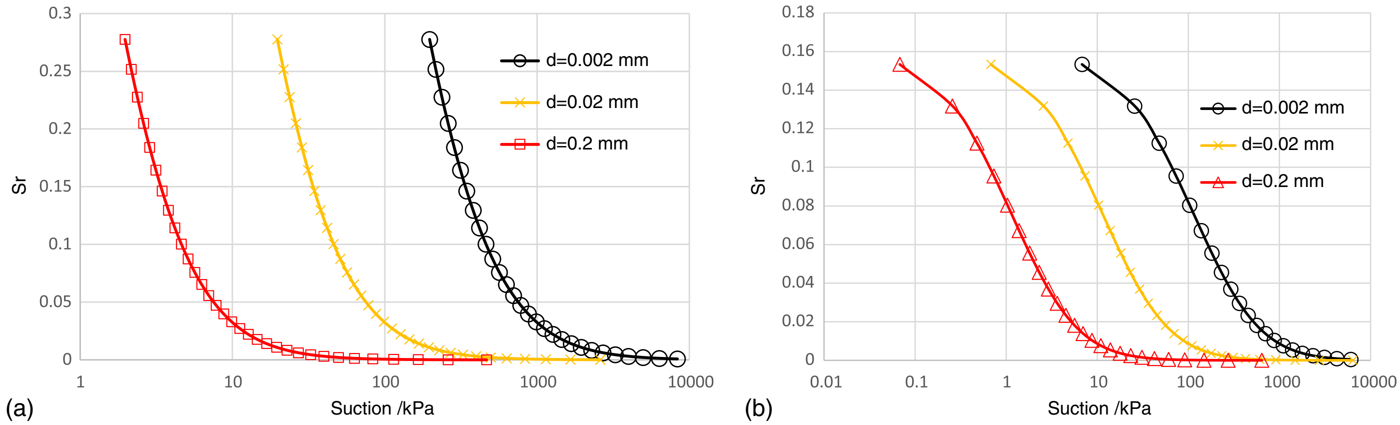

Fig. 5. Computed SWRC for Type A microstructure of saturation for monospheres of tetragonal packing of diameters 0.2, 0.02, and 0.002 mm: (a) contact angle 0°; and (b) contact angle 50°.

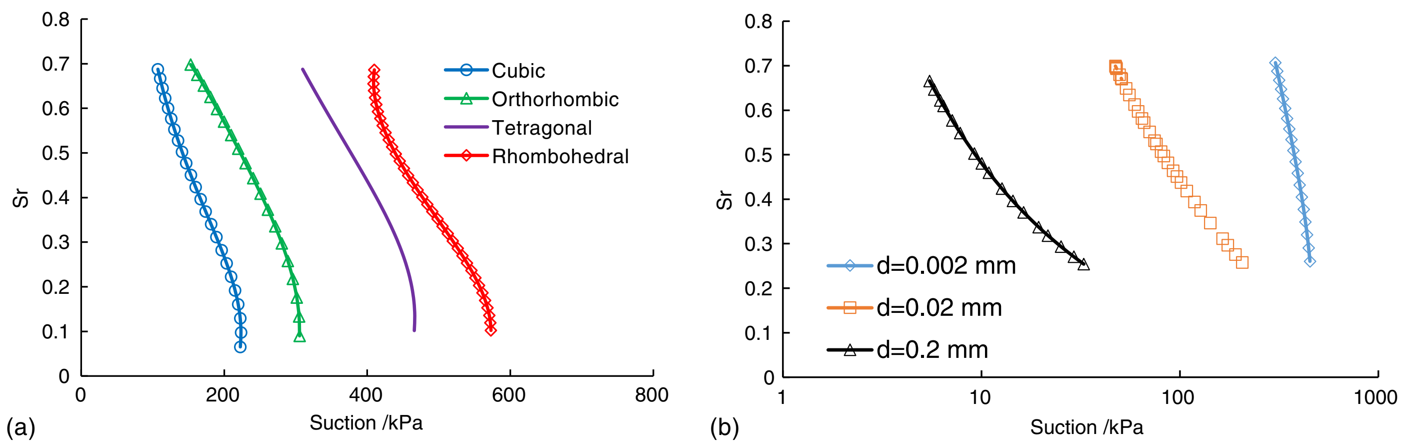

Fig. 6. Computed SWRC for Type B microstructure of saturation for monospheres: (a) different packing of diameter 0.002 mm; and (b) tetragonal-spheroidal packing of different diameters.

estimates of the p_s–S_r relationship. Taylor's equations for porosity (n) and specific surface area (S_s) for different packing configurations with a film of deposit on particles take the form

$$n = 1 - \frac{\pi}{\alpha_m}\left[\frac{2-m}{12}\left(\frac{2L_t}{d}\right)^3 + \frac{4-m}{8}\left(\frac{2L_t}{d}\right)^2 + \frac{1}{2}\left(\frac{2L_t}{d}\right) + \frac{1}{6}\right] \quad (23)$$

$$S_S = \frac{\pi}{\alpha_m d}\left[\frac{2-m}{2}\left(\frac{2L_t}{d}\right)^2 + \frac{4-m}{2}\left(\frac{2L_t}{d}\right) + 1\right] \quad (24)$$

where $\frac{2L_t}{d}$ = nondimensional film thickness; L_t = thickness of the film of water surrounding particles of diameter d; α_m = packing factor; and m is the number of contacts in a given packing arrangement (listed in Table 1). Eq. (23) gives the porosity of the assembly when all particles have been coated by a film of debris, which, in this study, is considered a film of water. At the same time, Eq. (24) may be interpreted as defining the area of water menisci S_{wm}. Thus, the degree of saturation corresponding to a given thickness of film of water as well as suction may be computed. Using this interpretation, Fig. 6 shows SWRC plots obtained from the previous equations for the grain size of 0.002 mm and different packing configurations.

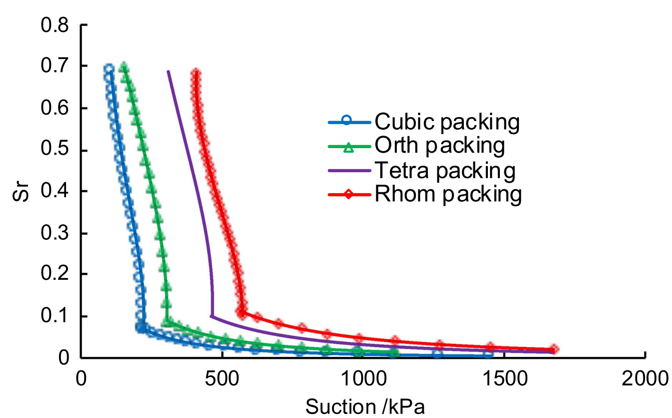

Fig. 7. Combined plot of computed SWRC for different packing monospheres of diameter 0.002 mm for contact angle 0°.

Fig. 7 shows a combined plot of the SWRC for pendular (contact angle 0°) as well as the thin film microstructure of saturation. The branch of the SWRC pertaining to pendular saturation is influenced by the contact angle, whereas the thin water film microstructure part of the SWRC is independent of it. A discontinuity in the gradient is clearly observed in the SWRC, which is indicative of a change in the microstructure of saturation.

The microstructure of saturation of Type A is likely to occur at quite low degrees of saturation. For suction to arise between monospheres, the filling angle is restricted to $(\pi/2–\theta)$. In view of this, for high values of the contact angle, the filling angle will be small, leading to low values of degrees of saturation. An interesting feature of Eq. (22) is that p_w can change sign from tensile to compressive. Convex shapes of water menisci [as observed in Lourenço et al. (2012)] can also arise. Thus, a pendular microstructure can occur when S_r becomes less than approximately 0.25, as indicated by Figs. 4 and 5. This may also be valid only in the drying phase and cannot be imagined to arise in the wetting phase.

The microstructure of Type B may be perceived as representative for S_r between 0.25 and 0.7. A discontinuity in the gradient of the SWRC is clearly seen in Fig. 7 and seems to be rational. However, another discontinuity in gradient is likely to take place when the microstructure changes from Type B to Type C (at approx. $S_r > 0.7$) as air flow becomes discontinuous. Discussion of the microstructure of Type C is beyond the scope of this paper.

Computation of SWRC from PSD or POSD

In the last three decades, several papers have been published on experimental identification as well as analytical approximation of the SWRC of soils. Initial work in the early 1980s was carried out by researchers in soil science, water management, and agricultural engineering whose interest was in diverse topics such as plant growth, nutrition, flood control, and river basin planning. In this section, we focus on determination of SWRCs of soils indirectly from PSD and POSD as well as from experiments. A method of computing POSD from PSD was first presented by Gupta and Larson (1979), followed by others (Arya and Paris 1981; Haverkamp and Parlange 1986). It uses porosity and specific gravity of soil particles. An empirical expression proposed by Van Genuchten (1980) involving three constants has been a subject of attention, and their values have been determined by a number of investigators for different types of soils. Numerous revisions and alternative expressions to the original formula have also been presented (Fredlund et al. 2002; Arya et al. 1999; Rezaee et al. 2011). In addition, tools of computational intelligence have been used to compute constants in many SWRC equations proposed, and software to convert PSD into a SWRC is also now available (Yang and You 2013; Schaap and Van Genuchten 2006).

On the experimental side of investigations, SWRC has been obtained by different techniques such as the pressure plate test (PPT) and mercury intrusion porosity (MIP). Recent techniques include high-resolution X-ray computer tomography to determine PSD. Finding the SWRC for a particular soil experimentally is time consuming as well as expensive. Moreover, there is considerable variation in the results obtained even when using the same technique, depending on the experimental setup (Alim et al. 2009; Nam et al. 2010) used. Interestingly, geotechnical engineers got interested in this area in 1990s because they were prompted by the need to incorporate SWRC in constitutive models of soils employed in finite-element codes.

Comparison of SWRC Characteristics Derived from PSD or POSD with Experiments

In this section, we compare the SWRCs of various soils computed from their respective gradation curves with those obtained from experiments. We restrict ourselves to experiments based on just one technique, that is, the axis translation method (Vanapalli et al. 2008; Wang et al. 2015, 2017), which is considered reliable for matric suctions up to a maximum value of 1,500 kPa. For comparison, we have chosen a low plasticity clay (CL) and a silty sand (SM) in Table 2 from a recent paper (Nam et al. 2010), where PSDs and SWRCs of several river bank sands were obtained from PPT as well as some in-situ test results.

The method of computation of SWRC is based on the method proposed by Arya and Paris (1981) and is described in the Appendix for completeness and clarity. In this research, it is assumed that all pores are interconnected. This assumption applies primarily to soils and not necessarily to all rocks where there can be "blind" (unconnected) pores as well as connected ones. Figs. 8 and 9 show PSDs and computed POSDs of these soils. Comparison of computed and experimentally observed SWRCs is shown in Fig. 10(a). Fig. 10(b) shows the variation of S_{wma} with degree of saturation for the two soils (for $T = 72 \times 10^{-6}$ kN/m). It is evident that a close correlation is obtained.

Table 2. Properties of two soils

Property	SM	CL
Void ratio	0.43	0.6
Specific gravity	2.69	2.72

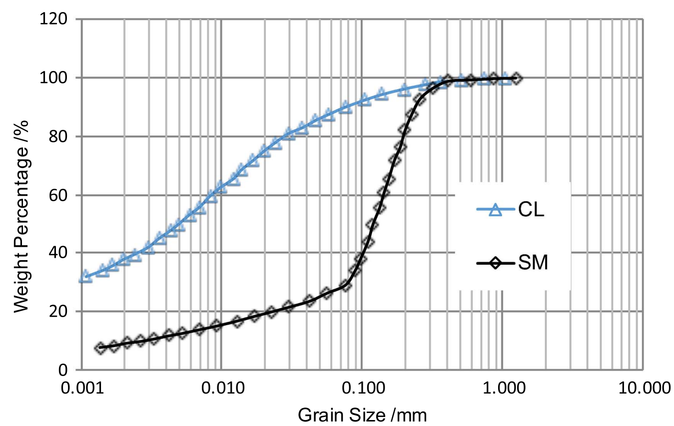

Fig. 8. Gradation curve of two soils chosen for computation of SWRC.

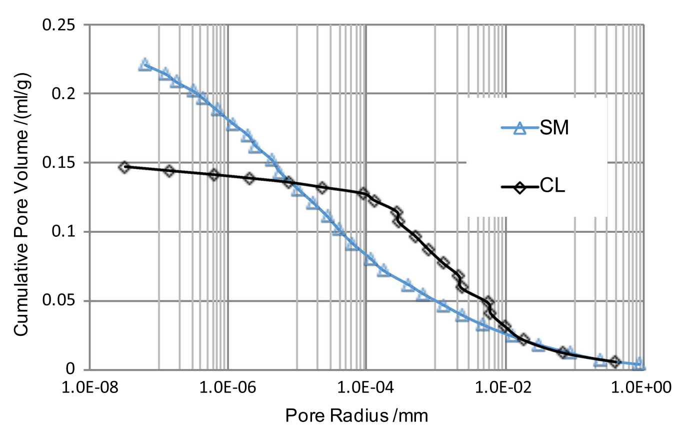

Fig. 9. Pore size distribution curve of two soils chosen for computation of SWRC.

Int. J. Geomech., 2020, 20(2): 04019159

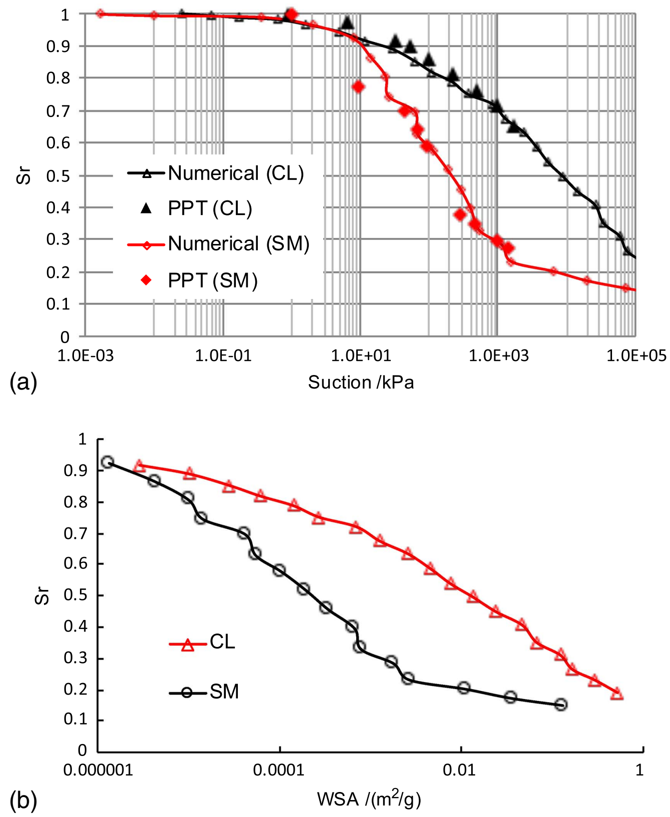

Fig. 10. (a) Computed SWRC with experimental results from PPT; and (b) interpreted S_{wma}.

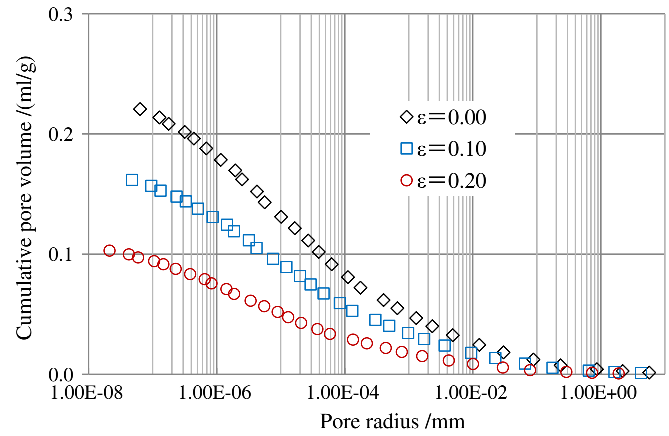

Fig. 11. POSD curves of the soil CL under different strains.

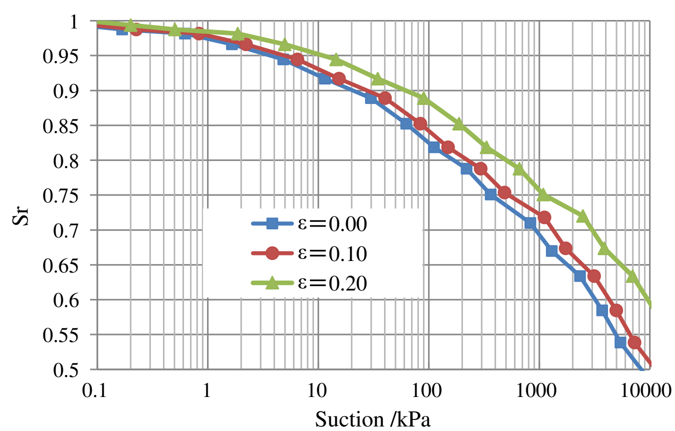

Fig. 12. SWRCs of the soil CL under different strains.

Derivation of Strain-Dependent SWRC

In the analysis of engineering structures in unsaturated soils, the influence of imposed strains on the SWRC has to be accounted for. It is extremely difficult to conduct tests like pressure plate tests with initial strains imposed on the soil sample. This was recognized long ago (Gallipoli et al. 2003b), and empirical equations for SWRC were proposed. Recently, a hypothesis relating to change in POSD as a result of strain was proposed for studying the pore fluid flow and permeability of deformable porous media by the first author of the current paper (Shin et al. 2015). The same hypothesis is applied here for determination of strain-dependent SWRC.

Hypothesis: Volumetric strain causes a uniform change in the diameter of the pores, which is proportional to its initial value. The overall change in POSD is such that a change in the void ratio corresponds to the magnitude of the imposed volumetric strain.

The previous hypothesis is not entirely intuitive. An analytical solution, which shows that the change in pore radius under hydrostatic stress or strain is linearly proportional to radius of the pore, has been derived using the theory of elasticity (Chau 2012). The same phenomenon was indirectly found from experimental results, which reported a linear relation between the pore size and isothermal compressibility of fluid-filled pores (Gor et al. 2015).

The variation of the void ratio at a certain level of ε_v can be determined from

$$\Delta e = -(1+e)\varepsilon_v / e \tag{25}$$

In this section, the previous hypothesis is directly employed to compute the evolution of POSD from PSD of soils under external loading. Recognizing that the soil moisture characteristic is essentially a pore-size distribution curve, the strain-dependent SWRC can be computed from the evolving POSD curves. Thus, incorporation of PSD in the constitutive model leads to a rational formulation for mechanical behavior of unsaturated soils. Figs. 11 and 12 show POSD and SWRC (water content versus suction) of the soil (CL) chosen for study at different strain conditions.

The framework of development of a constitutive model for unsaturated soils proposed here requires the specification of the water menisci area making contact with the air phase per unit volume (S_{wma}). Once SWRC has been derived from the PSD as shown previously, S_{wma} can be computed from Eq. (7). With S_{wma} determined as a function of S_r for a soil having a given gradation curve, and a methodology to modify it for the imposed strain at any point in the domain, description of the mechanical behavior of unsaturated soil is complete and is given by Eq. (20).

Numerical Simulation of the Mechanical Behavior of Two Unsaturated Soils Having the Same Characteristics Except Different Gradation Curves

The framework of treating unsaturated soil as a composite material, as presented earlier, is quite general, and any appropriate constitutive model for soil skeleton can be incorporated without any modifications; that is, there are no new constitutive parameters. The formulation simply extends the applicability of the existing models for the soil skeleton to unsaturated states at any degree of

Int. J. Geomech., 2020, 20(2): 04019159

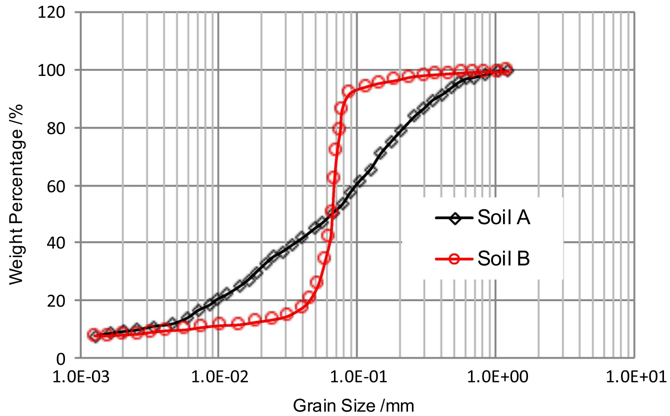

Fig. 13. Gradation curves of two hypothetical soils (Soils A and B).

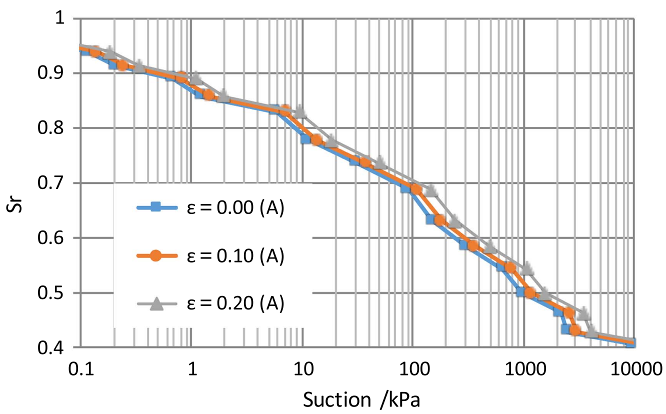

Fig. 14. SWRCs of Soil A under different strains.

saturation. The only additional input required is the gradation curve, which is readily available to the engineer as a part of site investigation report. The gradation curve can be in the form of discrete data points, that is, D_{10}, D_{30}, D_{50}, and so on.

The primary objective of this section is to demonstrate the influence of the gradation curve on the deformation and failure of unsaturated soils in triaxial compression tests with different initial conditions. Gradation curves influence the initial conditions of the unsaturated soil sample at the end of the consolidation phase. This difference arises due to existence of different S_{wma} leading to different initial values of suction. In drained or undrained tests at $S_r = 1$, suction does not arise; hence, the response is independent of the gradation curve.

For illustration, we chose two soils (A and B) with the same mechanical properties of soil skeleton, initial void ratios, and initial degree of saturation and different hypothetical gradation curves (Fig. 13). Computed SWRCs for the two soils based on their respective gradation curves are shown in Figs. 14 and 15. These figures also show SWRCs when an initial compressive volumetric strain of 10% is imposed on each of the soils. The SWRCs are seen to be widely different, making gradation curve an essential input parameter in unsaturated soil mechanics.

In the next numerical experiment, the two soils (A and B) were subjected to triaxial compression. The constitutive model adopted for both soils was a plasticity-based deviatoric hardening model (Pietruszczak 2010). Material parameters assumed for the soils adopted for simulations are

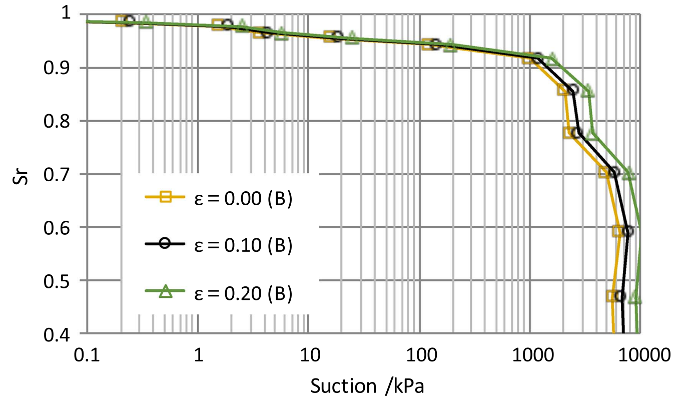

Fig. 15. SWRCs of Soil B under different strains.

$$K = 20\ \text{MPa}, \qquad G = 15\ \text{MPa}, \qquad \eta_f = \text{M} = 1.5,$$
$$\eta_c = 1.45, \qquad A = 0.002$$

where K and G = bulk and shear moduli, respectively; η_f and η_c = slopes of failure and zero dilatancy lines in q–p' space; and A = material parameter appearing in the hardening function. Let us consider now a sample of these soils with initial porosity $n_0 = 0.43$ and initial degrees of saturation $S_{r0} = 0.5$ and 0.6 tested at a confinement of $p' = 200$ kPa. Because the air phase is considered interconnected here, the initial air pressure is zero, which leads to $\mathrm{p}_w = -\beta = -970$ kPa for Soil A and -600 kPa for Soil B.

Fig. 16(a) shows q versus $\varepsilon_q = 2(\varepsilon_1 - \varepsilon_3)/3$ and (b) ε_v versus ε_q plots for the two soils. Fig. 16(c) shows the evolution of p_a and p_w. Under undrained conditions, both air and water are not allowed to escape from the sample. Results corresponding to drained as well as undrained conditions ($S_r = 1.0$) are also shown. It is evident that for unsaturated specimens, the strength is inversely proportional to S_r. Undrained and drained strengths are not influenced by the gradation curve. At the same time, it is clear that the gradation curve plays an important role in the mechanical behavior of unsaturated soils. This is simply because the surface area between the water and air interface on which surface tension forces act changes as it depends on the gradation curve.

Conclusions

Modeling of mechanical response of unsaturated soils is a challenging task for engineers involved in analysis of many types of critical structures. This is because the behavior of such soils depends on the microstructure of saturation and initial suction in the soil prior to application of a mechanical load. These factors must be taken into account in the analysis in an appropriate manner. In this paper, analytical expressions for the SWRC for idealized soil (monospheres of different packing) were derived for two different microstructures of saturation. These show a discontinuity in the gradient of the SWRC when the microstructure of saturation changes from the air phase being continuous to discontinuous.

Incorporation of the gradation curve has been proposed as a rational input to describe the mechanical response of unsaturated soils. It has been shown that suction as well as soil water retention characteristics can be determined, albeit with certain assumptions, from the gradation curve. Comparison of the computed SWRC with those obtained from the experiments indicates a reasonable agreement. It implies that assumptions made for obtaining the SWRC are rational and can be applied in engineering practice.

Int. J. Geomech., 2020, 20(2): 04019159

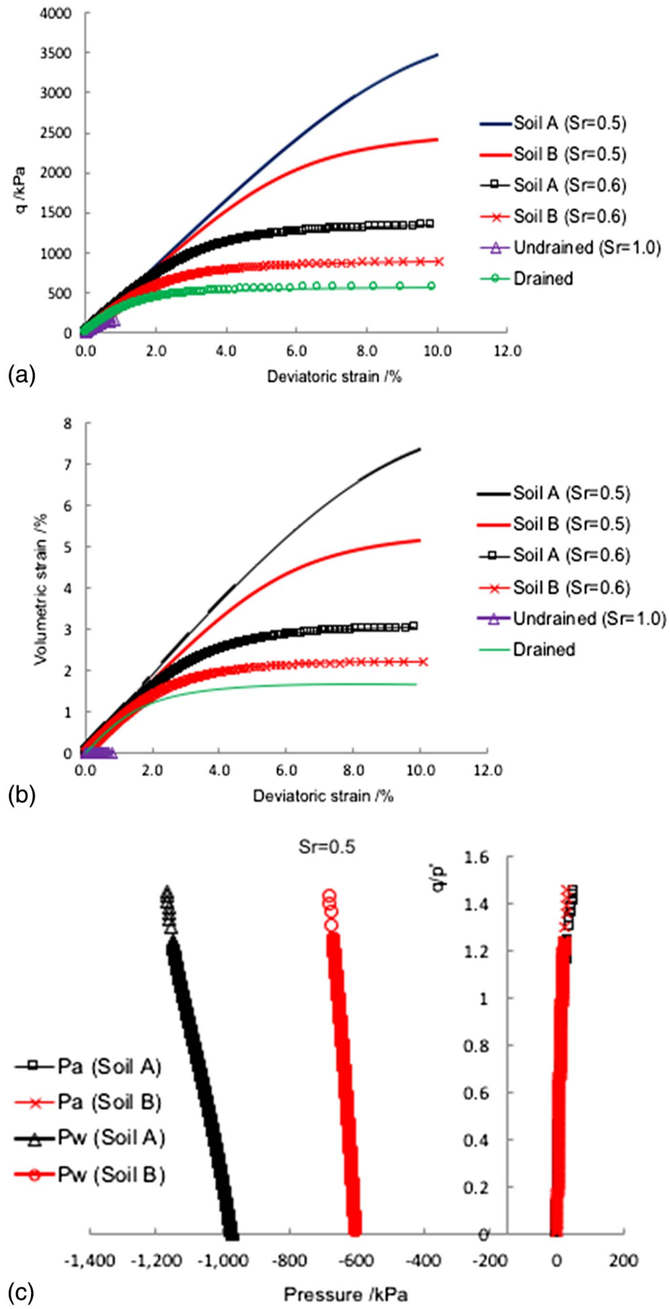

Fig. 16. (a) Deviatoric stress versus deviatoric strain in triaxial compression; (b) deviatoric strain (ε_q) versus volumetric strain (ε_v); and (c) evolution of pw and pa with q/p ($S_r = 0.5$).

It has been demonstrated that two soils with the same initial void ratio, degree of saturation, and mechanical parameters can have widely different mechanical strength and deformational characteristics depending on the gradation curves of the respective soils. It is therefore clear that gradation curve plays an important role in understanding of the mechanics of unsaturated soils.

Determination of the gradation curve of a soil is an established practice, and most site and laboratory investigation reports include this information as standard. Studies related to microstructure of saturation using various techniques such as X-ray computed tomography for different types of soils to determine specific surface area and evolution of water menisci area at various degrees of saturation would be useful and should be promoted. Experimental information on initial suction in samples after compaction, interpretation of contact angles, and adhesion of water in soils of known gradation curves is required to advance the research on a more rational basis.

Finally, SWRC characteristics may be viewed as a primary source of estimating the average surface area of air-water menisci for a given microstructure of saturation. This, in turn, is required for implementing the general constitutive framework as outlined in "Stress–strain Behavior of Unsaturated Soil Treated as a Composite Material."

Appendix. Computation of SWRC from PSD

First, the cumulative particle-size distribution curve is divided into a number of fractions, say, N. It is imagined that particles in each size fraction are of the same size, that is, average size and diameter. Assuming that the specific gravity of solid particles (G_s) for all N fractions is uniform, then the pore volume associated with each size fraction can be determined through the phase relationships (Arya and Paris 1981)

$$V_i = (W_i/G_s)e \tag{26}$$

where V_i = pore volume per unit mass associated with the solid particles in the ith particle size range; W_i = solid mass per unit mass in the ith particle size range; and e = void ratio.

Then, the cumulative degree of saturation S_r and water content w corresponding to the jth fraction can be calculated from

$$S_r = \frac{\sum_{i=1}^{j} V_i}{\sum_{k=1}^{N} V_k} \tag{27}$$

$$w = \frac{S_r e}{G_s} \tag{28}$$

Based on certain assumptions (Arya and Paris 1981): (1) the solid volume in any given assemblage can be approximated as that of uniform-size spheres defined by the mean particle radius for the fraction, and (2) the volume of the resulting pores can be approximated as that of uniform-size cylindrical capillary tubes whose radii are related to the mean particle radius for the fraction. The pore diameter of each range is characterized by the following empirical equation:

$$d_i = D_i[4en_i^{(1-\alpha)}/6]^{0.5} \tag{29}$$

where D_i and d_i = mean particle diameter and pore size corresponding to each size range, respectively; the model parameter α is to be determined empirically; and n_i = number of spherical particles in the ith particle size range and given as follows:

$$n_i \pi D_i^3/6 = W_i/G_s \tag{30}$$

By computing its value as a function of particle size for a number of the soil materials, Arya and Paris (1981) found that the values of α ranged from 1.35 to 1.39, and the value of 1.38 was considered the best estimate of α.

Then, the suction P_i corresponding to each pore size can be obtained from

$$P_i = -4T_s \cos\theta/d_i \tag{31}$$

where T_s = surface tension, and θ = contact angle between soil particles and the fluid, assumed as 0°.

Based on Eqs. (27)–(31), a program can be written to convert PSD to SWRC with PSD, specific gravity, and void ratio as the input data.

References

Alim, M., M. Nishigaki, L. P. Chegbeleh, J. A. Akudago, and M. Komatsu. 2009. "Determination of soil-water characteristic curves of unsaturated sandy soils using membrane filter with stainless wire mesh." *J. Faculty Environ. Sci. Technol.* 14 (1): 13–16.

Alonso, E. E., A. Gens, and A. Josa. 1990. "Constitutive model for partially saturated soils." *Geotechnique* 40 (3): 405–430. https://doi.org/10.1680/geot.1990.40.3.405.

Arya, L. M., F. J. Leij, M. T. van Genuchten, and P. J. Shouse. 1999. "Scaling parameter to predict the soil water characteristic from particle-size distribution data." *Soil Sci. Soc. Am. J.* 63 (3): 510–519. https://doi.org/10.2136/sssaj1999.03615995006300030013x.

Arya, L. M., and J. F. Paris. 1981. "A physicoempirical model to predict the soil moisture characteristic from particle-size distribution and bulk density data." *Soil Sci. Soc. Am. J.* 45 (6): 1023–1030. https://doi.org/10.2136/sssaj1981.03615995004500060004x.

Baker, R., and S. Frydman. 2009. "Unsaturated soil mechanics: Critical review of physical foundations." *Eng. Geol.* 106 (1): 26–39. https://doi.org/10.1016/j.enggeo.2009.02.010.

Barnes, G. E. 2010. *Soil mechanics: Principles and practice*. London: Palgrave Macmillan.

Beckett, C. T., and C. E. Augarde. 2013. "Prediction of soil water retention properties using pore-size distribution and porosity." *Can. Geotech. J.* 50 (4): 435–450. https://doi.org/10.1139/cgj-2012-0320.

Chau, K. -T. 2012. *Analytic methods in geomechanics*, P108. Boca Raton, FL: CRC Press.

Chen, Z.-H., D. Fredlund, and J. K. Gan. 1999. "Overall volume change, water volume change, and yield associated with an unsaturated compacted loess." *Can. Geotech. J.* 36 (2): 321–329. https://doi.org/10.1139/t98-097.

Cooke, A. J., and R. K. Rowe. 1999. "Extension of porosity and surface area models for uniform porous media." *J. Environ. Eng.* 125 (2): 126–136. https://doi.org/10.1061/(ASCE)0733-9372(1999)125:2(126).

Craig, R. F. 2013. *Soil mechanics*. New York: Springer.

Dieudonné, A.-C., S. Levasseur, R. Charlier, G. Della Vecchia, and C. Jommi. 2013. "A water retention model for compacted clayey soils." In *Proc., Computational Geomechanics ComGeo III*, 23–30. Rhodes, Greece: International Centre for Computational Engineering.

Fredlund, D. G., and H. Rahardjo. 1993. *Soil mechanics for unsaturated soils*. New York: Wiley.

Fredlund, M. D., G. W. Wilson, and D. G. Fredlund. 2002. "Use of the grain-size distribution for estimation of the soil-water characteristic curve." *Can. Geotech. J.* 39 (5): 1103–1117. https://doi.org/10.1139/t02-049.

Frydman, S., and R. Baker. 2009. "Theoretical soil-water characteristic curves based on adsorption, cavitation, and a double porosity model." *Int. J. Geomech.* 9 (6): 250–257. https://doi.org/10.1061/(ASCE)1532-3641(2009)9:6(250).

Gallipoli, D., A. Gens, R. Sharma, and J. Vaunat. 2003a. "An elasto-plastic model for unsaturated soil incorporating the effects of suction and degree of saturation on mechanical behaviour." *Géotechnique* 53 (1): 123–135. https://doi.org/10.1680/geot.2003.53.1.123.

Gallipoli, D., S. Wheeler, and M. Karstunen. 2003b. "Modelling the variation of degree of saturation in a deformable unsaturated soil." *Géotechnique* 53 (1): 105–112. https://doi.org/10.1680/geot.2003.53.1.105.

Gor, G. Y., D. W. Siderius, C. J. Rasmussen, W. P. Krekelberg, V. K. Shen, and N. Bernstein. 2015. "Relation between pore size and the compressibility of a confined fluid." *J. Chem. Phys.* 143 (19): 194506. https://doi.org/10.1063/1.4935430.

Gupta, S., and W. Larson. 1979. "Estimating soil water retention characteristics from particle size distribution, organic matter percent, and bulk density." *Water Resour. Res.* 15 (6): 1633–1635. https://doi.org/10.1029/WR015i006p01633.

Haverkamp, R., and J.-Y. Parlange. 1986. "Predicting the water-retention curve from particle size distribution: Sandy soils without organic matter." *Soil Sci.* 142 (6): 325–339. https://doi.org/10.1097/00010694-198612000-00001.

Hu, R., Y. Chen, H. Liu, and C. Zhou. 2013. "A water retention curve and unsaturated hydraulic conductivity model for deformable soils: Consideration of the change in pore-size distribution." *Geotechnique* 63 (16): 1389. https://doi.org/10.1680/geot.12.P.182.

Imre, E., K. Rajkai, T. Firgi, I. Laufer, R. Genovese, and C. Jommi. 2012. "Modified grading curve–SWCC relations." In *Unsaturated soils: Research and applications*, 39–46. Berlin: Springer.

Khalili, N., M. A. Habte, and S. Zargarbashi. 2008. "A fully coupled flow deformation model for cyclic analysis of unsaturated soils including hydraulic and mechanical hystereses." *Comput. Geotech.* 35 (6): 872–889. https://doi.org/10.1016/j.compgeo.2008.08.003.

Khalili, N., and M. Khabbaz. 1998. "A unique relationship of chi for the determination of the shear strength of unsaturated soils." *Geotechnique* 48 (5): 681–687. https://doi.org/10.1680/geot.1998.48.5.681.

Khoshghalb, A., A. Y. Pasha, and N. Khalili. 2015. "A fractal model for volume change dependency of the water retention curve." *Géotechnique* 65 (2): 141–146. https://doi.org/10.1680/geot.14.T.016.

Lian, G., C. Thornton, and M. J. Adams. 1993. "A theoretical study of the liquid bridge forces between two rigid spherical bodies." *J. Colloid Interface Sci.* 161 (1): 138–147. https://doi.org/10.1006/jcis.1993.1452.

Lim, Y. Y., and G. A. Miller. 2004. "Wetting-induced compression of compacted Oklahoma soils." *J. Geotech. Geoenviron. Eng.* 130 (10): 1014–1023. https://doi.org/10.1061/(ASCE)1090-0241(2004)130:10(1014).

Lourenço, S., D. Gallipoli, C. E. Augarde, D. G. Toll, P. C. Fisher, and A. Congreve. 2012. "Formation and evolution of water menisci in unsaturated granular media." *Geotechnique* 62 (3): 193. https://doi.org/10.1680/geot.11.P.034.

Mehrotra, V., and K. Sastry. 1980. "Pendular bond strength between unequal-sized spherical particles." *Powder Technol.* 25 (2): 203–214. https://doi.org/10.1016/0032-5910(80)87031-8.

Molenkamp, F., and A. Nazemi. 2003. "Interactions between two rough spheres, water bridge and water vapour." *Geotechnique* 53 (2): 255–264. https://doi.org/10.1680/geot.2003.53.2.255.

Nam, S., M. Gutierrez, P. Diplas, J. Petrie, A. Wayllace, N. Lu, and J. J. Muñoz. 2010. "Comparison of testing techniques and models for establishing the SWCC of riverbank soils." *Eng. Geol.* 110 (1): 1–10. https://doi.org/10.1016/j.enggeo.2009.09.003.

Ng, C. W., and B. Menzies. 2007. *Advanced unsaturated soil mechanics and engineering*. Boca Raton, FL: CRC Press.

Ning, L., and W. J. Likos. 2004. *Unsaturated soil mechanics*. Hoboken, NJ: Wiley.

Pande, G., and S. Pietruszczak. 2015. "On unsaturated soil mechanics—Personal views on current research." *Stud. Geotech. Mech.* 37 (3): 73–84. https://doi.org/10.1515/sgem-2015-0035.

Pasha, A. Y., A. Khoshghalb, and N. Khalili. 2017. "Hysteretic model for the evolution of water retention curve with void ratio." *J. Eng. Mech.* 143 (7): 04017030. https://doi.org/10.1061/(ASCE)EM.1943-7889.0001238.

Pedroso, D. M., and M. M. Farias. 2011. "Extended Barcelona basic model for unsaturated soils under cyclic loadings." *Comput. Geotech.* 38 (5): 731–740. https://doi.org/10.1016/j.compgeo.2011.02.004.

Pereira, J. H., and D. G. Fredlund. 2000. "Volume change behavior of collapsible compacted gneiss soil." *J. Geotech. Geoenviron. Eng.* 126 (10): 907–916. https://doi.org/10.1061/(ASCE)1090-0241(2000)126:10(907).

Pietruszczak, S. 2010. *Fundamentals of plasticity in geomechanics*. Leiden, Netherlands: CRC Press.

Pietruszczak, S., and G. Pande. 1991. "On the mechanics of partially saturated soils." *Comput. Geotech.* 12 (1): 55–71. https://doi.org/10.1016/0266-352X(91)90011-4.

Pietruszczak, S., and G. Pande. 1995. "On the mechanical response of partially saturated soils at low and high degrees of saturation." In Vol. 5 of *Numerical models in geomechanics*, 32–38. Leiden, Netherlands: A.A. Balkema.

Pietruszczak, S., and G. Pande. 1996. “Constitutive relations for partially saturated soils containing gas inclusions.” *J. Geotech. Eng.* 122 (1): 50–59. https://doi.org/10.1061/(ASCE)0733-9410(1996)122:1(50).

Rezaee, L., M. Shabanpour, and N. Davatgar. 2011. “Estimating the soil water retention curve from soil particle size distribution using the Arya and Paris model for Iranian soils.” *Turk. J. Agric. For.* 35 (6): 649–657. https://doi.org/10.3906/tar-1006-1095.

Romero, E., and P. H. Simms. 2008. “Microstructure investigation in unsaturated soils: A review with special attention to contribution of mercury intrusion porosimetry and environmental scanning electron microscopy.” In *Laboratory and field testing of unsaturated soils*, 93–115. New York: Springer.

Schaap, M. G., and M. T. Van Genuchten. 2006. “A modified Mualem–van Genuchten formulation for improved description of the hydraulic conductivity near saturation.” *Vadose Zone J.* 5 (1): 27–34. https://doi.org/10.2136/vzj2005.0005.

Schanz, T. 2007. *Experimental unsaturated soil mechanics*. New York: Springer.

Shin, H. S., K. Y. Kim, and G. N. Pande. 2015. “On computation of strain-dependent permeability of rocks and rock-like porous media.” *Int. J. Numer. Anal. Methods Geomech.* 39: 821–832. https://doi.org/10.1002/nag.2334.

Shin, H.-S., K.-Y. Kim, and G. N. Pande. 2013. “Porosity and pore-size distribution of geomaterials from X-ray CT scans.” In *Multiphysical testing of soils and shales*, 177–186. Berlin: Springer.

Tarantino, A. 2009. “A water retention model for deformable soils.” *Géotechnique* 59 (9): 751–762. https://doi.org/10.1680/geot.7.00118.

Taylor, S. W. 1990. “Transport of substrate and biomass in pourous media with application to in-situ bioremediation of organic contaminants in groundwater.” Ph.D. dissertation, Dept. of Civil Engineering, Princeton Univ.

Taylor, S. W., and P. R. Jaffé. 1990. “Biofilm growth and the related changes in the physical properties of a porous medium: 3. Dispersivity and model verification.” *Water Resour. Res.* 26 (9): 2171–2180. https://doi.org/10.1029/WR026i009p02171.

Terzaghi, K. V. 1936. “The shearing resistance of saturated soils and the angle between the planes of shear.” In *Proc., 1st Int. Conf. on Soil Mechanics and Foundation Engineering*, 54–56. Cambridge, MA: Harvard University Press.

Vanapalli, S. K., M. Nicotera, and R. S. Sharma. 2008. “Axis translation and negative water column techniques for suction control.” *Geotech. Geol. Eng.* 26 (6): 645. https://doi.org/10.1007/s10706-008-9206-3.

Van Genuchten, M. T. 1980. “A closed-form equation for predicting the hydraulic conductivity of unsaturated soils.” *Soil Sci. Soc. Am. J.* 44 (5): 892–898. https://doi.org/10.2136/sssaj1980.03615995004400050002x.

Wang, M., L. Kong, and M. Zang. 2015. “Effects of sample dimensions and shapes on measuring soil–water characteristic curves using pressure plate.” *J. Rock Mech. Geotech. Eng.* 7 (4): 463–468. https://doi.org/10.1016/j.jrmge.2015.01.002.

Wang, M., G. Pande, L. Kong, and Y. Feng. 2017. “Comparison of pore-size distribution of soils obtained by different methods.” *Int. J. Geomech.* 17 (1): 06016012. https://doi.org/10.1061/(ASCE)GM.1943-5622.0000696.

Wheeler, S., D. Gallipoli, and M. Karstunen. 2002. “Comments on use of the Barcelona basic model for unsaturated soils.” *Int. J. Numer. Anal. Methods Geomech.* 26 (15): 1561–1571. https://doi.org/10.1002/nag.259.

Wheeler, S., R. Sharma, and M. Buisson. 2003. “Coupling of hydraulic hysteresis and stress–strain behaviour in unsaturated soils.” *Geotechnique* 53 (1): 41–54. https://doi.org/10.1680/geot.2003.53.1.41.

Yang, X., and X. You. 2013. “Estimating parameters of van Genuchten model for soil water retention curve by intelligent algorithms.” *Appl. Math.* 7 (5): 1977–1983. https://doi.org/10.12785/amis/070537.

Yu, Y., and R. Kerry Rowe. 2012. “Improved solutions for porosity and specific surface of a uniform porous medium with attached film.” *J. Environ. Eng.* 138 (4): 436–445. https://doi.org/10.1061/(ASCE)EE.1943-7870.0000480.

Zhang, X. 2016. “Limitations of suction—Controlled triaxial tests in the characterization of unsaturated soils.” *Int. J. Numer. Anal. Methods Geomech.* 40 (2): 269–296. https://doi.org/10.1002/nag.2401.